Appendix A

Ruthenium Olefin Metathesis Catalysts Bearing Carbohydrate-Based N-Heterocyclic Carbenes

The text in this appendix is reproduced in part with permission from:

Keitz, B. K.; Grubbs, R. H. *Organometallics* **2010**, *29*, 403.

Copyright 2009 American Chemical Society

Introduction

As discussed in Chapter 1, the development of powerful, air-stable catalysts has made olefin metathesis an indispensable tool in a variety of fields. Recently, efforts to improve catalyst stability and activity have focused on modifications to the N-heterocyclic carbene (NHC).[1] In general, *N*-aryl bulk was found to increase activity while increased backbone substitution decreased activity but increased catalyst lifetime.[2] However, these structural studies were limited to catalysts with NHCs containing *N*-aryl substituents. NHC-based metathesis catalysts with *N*-akyl groups on the other hand have received relatively little attention due to their lower stability in solution and generally lower activity.[3,4] This lower activity was rationalized in Chapters 4 and 5. However, certain N-alkyl NHC-based catalysts have demonstrated remarkable activity, including the traditionally difficult RCM of tetrasubstituted olefins.[5]

One class of N-alkyl substituents for NHCs which have not yet been explored for metathesis applications are carbohydrates. Carbohydrates are extremely abundant molecules and comprise some of the most important biological machinery in living organisms including glycolipids, glycoproteins, and nucleic acids. Thus, it is no surprise that their synthesis[6] and their biological function continue to be studied extensively.[7] As ligands, carbohydrates are advantageous because of their innate chirality and steric bulk in addition to their long history of synthetic manipulation and solubility in water. Indeed, carbohydrates have already shown promise as ligands for asymmetric catalysis[8] and as chiral synthons.[9] Additionally, carbohydrates have also been used as ligand scaffolding for platinum and other metals.[10] Finally,

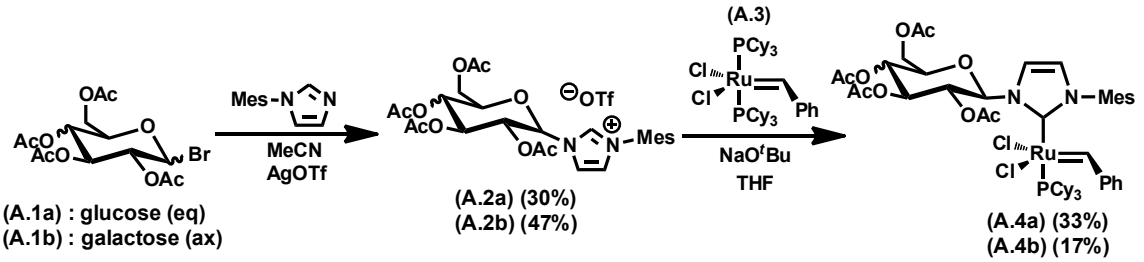

Figure A.1. Preparation of catalysts **A.4a** and **A.4b**

carbohydrates possess multiple, modular stereocenters and a steric environment which can be tuned through the judicious choice of alcohol protecting groups. However, carbohydrate-based NHCs have only recently been synthesized, and, to the best of our knowledge, a rigorous study of their applications in transition metal catalysis or organocatalysis has not been undertaken.[15] Therefore, with the goals of developing a new structural class of highly active, stable, stereoselective olefin metathesis catalysts, and determining the potential of carbohydrate-based NHCs in catalysis, we undertook the synthesis of catalysts containing carbohydrate-based NHCs.

Results and Dicussion

Several groups have demonstrated that a carbohydrate containing imidazolium salt may be synthesized from the reaction of an alkyl or aryl imidazole with glucopyranosyl bromide.[11] Along these lines, imidazolium salts **A.2a** and **A.2b** were synthesized in acceptable yields from the reaction of mesityl imidazole with 2,3,4,6-tetra-*O*-acetyl-α-D-glucopyranosyl bromide (**A.1a**) or 2,3,4,6-tetra-*O*-acetyl-α-D-galactopyranosyl bromide (**A.1b**), respectively, in the presence of silver triflate according to a previous report (Figure A.1).[15] Subsequent deprotonation with

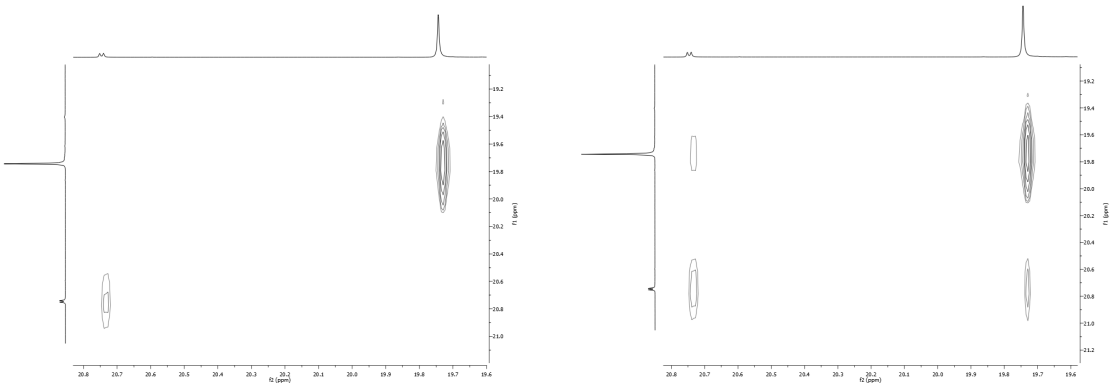

Figure A.2. 600 MHz ^{1}H NMR NOESY for the benzylidene region of **A.4a** in C_6D_6 at 25 °C. Mixing time = 0 ms (left) and 100 ms (right). Peak intensities are listed clockwise starting at the high field diagonal resonance. Left—589.02, 49.36. Right —1047.03, 71.91, 68.03, 30.99

sodium *tert*-butoxide and reaction with catalyst **A.3** in THF afforded the desired complex (**A.4a**) following column chromatography on silica gel. Complex **A.4a** was isolated as a single anomer (β) while **A.4b** (along with **A.2b**) was isolated as a ca. 1.2:1 mixture of β:α anomers.[12] Other methods of NHC ligation including deprotonation with KHMDS or transmetalation from a silver complex[13] failed to give significant yields of **A.4a/b**.[14] Both **A.4a** and **A.4b** were bench stable in the solid state and could be stored as a solution in C_6H_6 under a nitrogen or argon atmosphere for a period of at least 3 days as determined by ^{1}H NMR spectroscopy.

Characterization of complex **A.4a** at 25 °C revealed the unusual presence of two benzylidene resonances at ca. 19.77 (s) and 20.78 (d) ppm in the ^{1}H NMR spectrum (C_6D_6), both of which were correlated to the main ruthenium complex. Interestingly, the benzylidene resonances were found to exchange with one another using a 2D-NOESY experiment (Figure A.2). Based on the spin multiplicities of these peaks, along with the 2D-NOESY spectrum, the observed exchange was

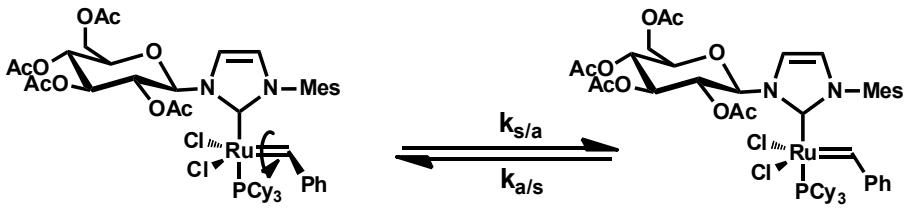

Figure A.3. Equilibrium depicting rotation about Ru – C/benzylidene bond with anti/syn designation denoting relative position of benzylidene phenyl group to the NHC

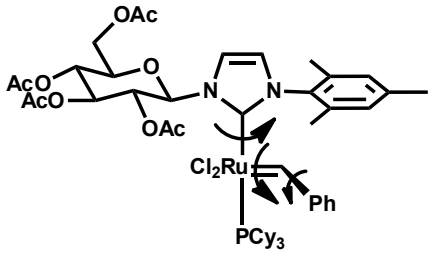

Figure A.4. Summary of rotational processes in complex **A.4a**

attributed to two rotameric species resulting from rotation about the benzylidene C–Ru bond (Figure A.3). At room temperature, such a process is more common among molybdenum and tungsten metathesis catalysts[15] but has also been observed for Ru-based catalysts.[16]

Alkylidene rotamers are not just structural curiosities, but also play an important role in the activity and selectivity of metathesis catalysts.[19] Unfortunately, a crystal structure of either rotamer of **A.4a** was unobtainable despite a variety of crystallization conditions. Therefore, in order to fully characterize the unique properties of **A.4a**, a more in-depth structural study of the rotamers of **A.4a** in solution was conducted using NMR spectroscopy.

Cooling a CD_2Cl_2 solution of **A.4a** to –75 °C resulted in the freezing out of the benzylidene C–Ru bond rotation as well as the appearance of a new benzylidene resonance which can be attributed to slow rotation about the Ru–NHC bond (see

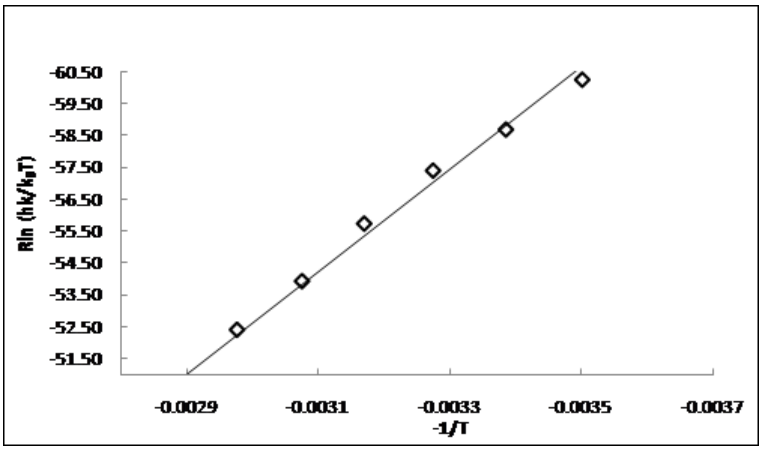

Figure A.5. Eyring plot showing VT-NMR spectroscopy data for complex **A.4a**. R^2= 0.989, $\Delta H^{\ddagger}$ = 16.1±0.8 kcal/mol, $\Delta S^{\ddagger}$ = -4.4±2.5 cal/(mol•K)

Experimental).[17] Moreover, at this temperature, the benzylidene *ortho* protons also became well resolved, indicating that rotation about the C(carbene)–C(phenyl) bond is facile at RT. A graphical summary of observable dynamic processes in **A.4a** at 25 °C is shown in Figure A.4.[18]

From a magnetization transfer experiment[19] conducted at 25 °C, $k_{s/a}$ and $k_{a/s}$ for the benzylidene rotamers were determined to be 1.01 s^{-1} and 5.28 s^{-1}, respectively.[20] These values correspond to a $\Delta G^{\ddagger}$ of 17.42 kcal/mol for the forward reaction (syn to anti) which is consistent with previous reports of Ru– C/benzylidene rotation and also with the relative site population observed at 25 °C.[20] Furthermore, a VT ^{1}H NMR spectroscopy experiment with subsequent line shape analysis (see Experimental) yielded a value of 17.4 ± 0.2 kcal/mol for $\Delta G^{\ddagger}$ at 25 °C, consistent with the value obtained from the magnetization transfer experiment (Figure A.5). The ^{1}H NMR spectrum of complex **A.4b** looked qualitatively similar to that of **A.4a** although no attempt was made to determine the kinetic parameters quantitatively. These results demonstrate the structural rigidity of **A.4a** compared to other Ru-

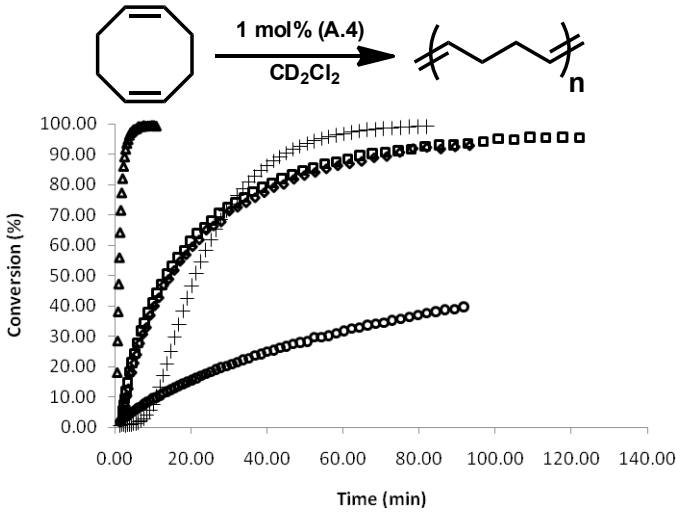

Figure A.6. Conversion of COD with catalyst **A.3** (circles), **A.6** (triangles), **A.5** (crosses), **A.4a** (square,1 mol%), and **A.4b** (diamond, 1 mol%). Conditions were 1000:1 monomer to catalyst ratio in CD_2Cl_2 (0.1 M in monomer) at 30 °C.

based metathesis catalysts where bond rotation is more facile at 25 °C.[20b]

Following characterization, both **A.4a** and **A.4b** were subjected to a series of standard reactions for ROMP, RCM, and CM in order to evaluate their activity and selectivity compared with previously reported catalysts.[29] Additionally, the effectiveness of **A.4a/b** at asymmetric reactions was also of particular interest considering the chiral nature of the carbohydrate ligand. Therefore, asymmetric ring-opening cross metathesis (AROCM) was chosen as a means of evaluating the performance of **A.4a/b** in asymmetric reactions.

The ROMP of strained olefinic ring systems is one of the earliest industrial applications of olefin metathesis and remains a popular tool for modern polymer synthesis.[1] The effectiveness of catalysts **A.4a/b** at ROMP was examined by measuring the rate of polymerization of cyclooctadiene (COD) (Figure A.6). Despite a relatively slow initiation, both catalysts were able to reach >95% conversion

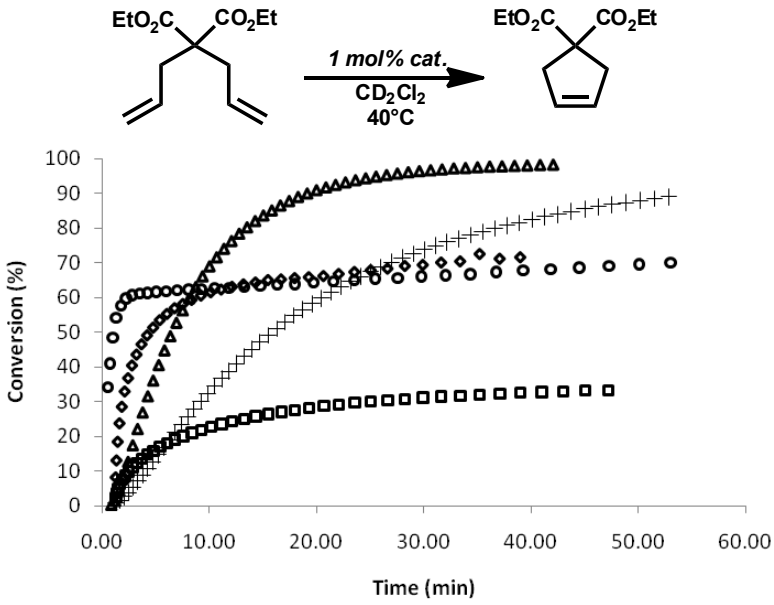

Figure A.7. RCM conversion of DEDAM with catalysts **A.3** (circles), **A.6** (triangles), **A.5** (crosses), **A.4a** (squares), and **A.4b** (diamonds). Conditions were 1 mol% catalyst, 0.1 M in substrate CD_2Cl_2 at 40 °C for **A.4a** and **A.4b** and at 30 °C for **A.3**, **A.6**, and **A.5**.

within 2 h at 30 °C with an initial monomer to catalyst ratio of 100:1. As expected, both **A.4a** and **A.4b** showed similar kinetic behavior. Additionally, both **A.4a**/**b** performed well compared with other metathesis catalysts, showing a much higher activity than phosphine-based catalyst **A.3** and similar activity to $(Imes)Cl_2Ru{=}CHPh$ (**A.5**). On the other hand, **8a/b** were less active than catalyst $(H_2IMes)Cl_2Ru{=}CHPh$ (**A.6**) which contains a completely saturated NHC ligand.[21]

Norbornene-based substrates and cyclooctene (COE) could also be polymerized effectively using **A.4a/b** with norbornene monomers showing an increase in rate due to the increase in ring strain. Characterization of the isolated polymers by GPC revealed high PDIs and molecular weights much larger than predicted which suggests a relatively slow catalyst initiation step compared to what

is observed for fast initiating catalysts such as **A.6** or its bis-pyridine derivative.[22]

Given the good activity of the catalysts in ROMP, we next focused on testing their activity in RCM, which is generally a more demanding reaction for catalysts than ROMP.[1] A standard reaction for testing the RCM activity of a particular catalyst is the ring closing of diethyl diallyl malonate (DEDAM) to the cyclopentene product (Figure A.7).[29] Interestingly, **A.4a** and **A.4b** showed reproducibly different kinetic behavior when exposed to DEDAM even though they only differ at one stereocenter (C4).[23] It is possible that the distinct behavior is due to one catalyst being more susceptible to a particular decomposition pathway. Another possibility is that the α anomer, which is observed in **A.4b** but not **A.4a**, is much more reactive than the β anomer under these specific reaction conditions.

At a catalyst loading of 1 mol%, both **A.4a** and **A.4b** showed good performance during the RCM of DEDAM compared with catalysts **A.6** and **A.5**, while **A.4b** displayed similar activity to catalyst **A.3**. Further reaction times or heating did not improve conversion significantly, but better results were achieved by increasing the catalyst loading to 5 mol% (not shown). Although we have not isolated any catalyst decomposition products, the early catalyst death of **A.4a/b** during RCM indicates that the catalysts are particularly susceptible to decomposition pathways involving methylidene intermediates, similar to catalyst **A.3**.[24]

Cross metathesis, in contrast to ROMP and RCM, does not possess as strong a driving force that pushes the metathesis reaction to completion. Additionally, secondary metathesis events often change the stereochemistry of the desired product, eventually resulting in an excess of the thermodynamically more stable *E*

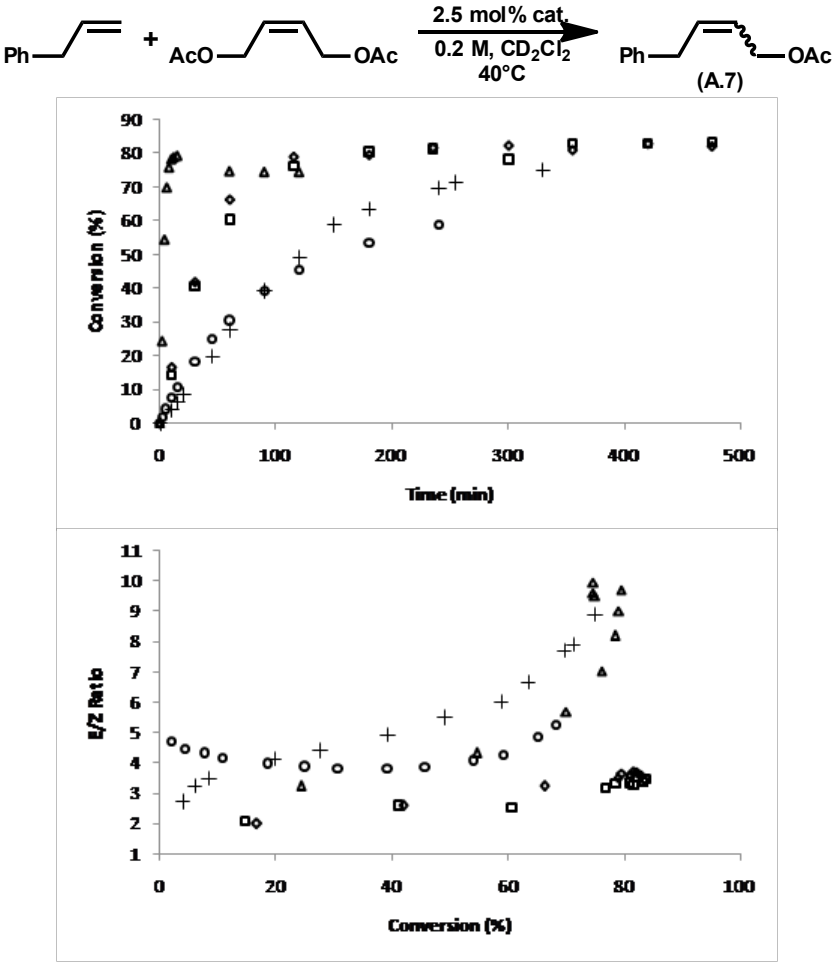

Figure A.8. Conversion to desired cross product **A.7** and E/Z ratio using **A.3** (circles), **A.6** (triangles), **A.5** (crosses), **A.4a** (squares), and **A.4b** (diamonds). Data for **A.3**, **A.6**, and **A.5** obtained at 30 °C. E/Z ratio and conversion determined by GC relative to tridecane standard.

product. Combined, these challenges often result in reactions with low yield and low selectivity. Controlling the stereochemistry of the olefin product in particular has been extraordinarily challenging although progress in this area is being made.[25]

In order to evaluate the activity and selectivity of catalysts **A.4a/b**, the CM of allylbenzene and *cis*-diacetoxybutene was studied.[26] The formation of all reaction products including the desired cross product (**A.7**), *trans*-diacetoxybutene, and the *E* and *Z* isomers of the homocoupled allylbenzene were monitored over time via

Table A.1. AROCM with catalysts **A.4a/b**[a]

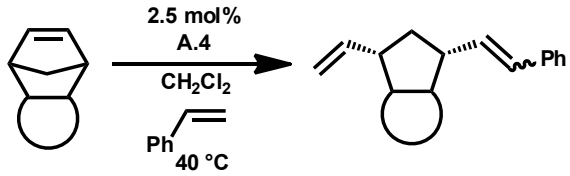

Entry	Substrate	Catalyst	Solvent	Time (h)	ee % E(Z)[a]	Yield % (E:Z)[b]
1	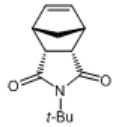	**A.4a**	CH_2Cl_2	8	11 (7)	43 (1.3:1)
		A.4a	Toluene	15	20 (7)	88 (2.7:1)
		A.4b	Toluene	15	11(3)	86 (1.4:1)
2	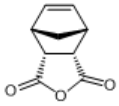	**A.4a**	CH_2Cl_2	15	22 (n.d.)	36 (n.d.)
		A.4a	Toluene	15	26 (n.d.)	80 (n.d.)
		A.4b	Toluene	15	19 (n.d.)	73 (n.d.)
3		**A.4a**	Toluene	10	75 (4)	8 (2.7:1)
4		**A.4a**	Toluene	5	20 (4)	64 (0.7:1)

[a] ee% determined by chiral HPLC. [b] isolated yield after column chromatography.

GC (Figure A.8). Catalysts **A.4a/b** reached similar levels of conversion compared with **A.3**, **A.6**, and **A.5** but maintained an exceptional *E/Z* ratio of around 3. Such a low *E/Z* ratio is unusual at high conversions where secondary metathesis events begin to favor the thermodynamic product. Furthermore, this result is also significant because the only difference between **A.5** and **A.4a/b** is the replacement of a mesityl group with a carbohydrate, indicating that carbohydrates can have a substantial effect on catalyst selectivity. However, the low *E/Z* ratio appears to be more a result of catalyst decomposition as opposed to an inherent preference for one isomer over the other since adding a fresh batch of catalyst caused the *E/Z* ratio to increase to ca. 8 over a period of 5 h. No differences in either conversion

or *E/Z* ratio were observed for catalysts **A.4a** and **A.4b**.

A relatively recent application of ruthenium-based olefin metathesis is the AROCM of substituted norbornenes with terminal olefins.[31] Given the relative selectivity observed during CM and the chiral nature of the sugar moiety attached to the NHC ligand, AROCM was attempted with the hope of observing enantiomeric selectivity. Exposing a variety of norbornene-based substrates to catalysts **A.4a/b** in the presence of styrene for several hours at 40 °C resulted in complete conversion to the desired *cis* and *trans* products. As shown in Table A.1, reactions performed in toluene generally outperformed those conducted in methylene chloride in terms of yield due to the greater long-term stability of the catalysts in nonchlorinated solvents.[27] Isolated yields were generally excellent while ee's were poor compared to previously reported ruthenium-based catalysts.[28] The extremely low yield and relatively high ee of entry 3 in Table 1 appears to be an anomaly that is specific to that substrate.[31c] Substrates from entries 3 and 4 were not tested with **A.4b** due to their relatively low isolated yield. Despite the modest levels of enantioselectivity observed, these results demonstrate the potential of carbohydrate-based ligands as tools for asymmetric catalysis. Furthermore, the variety of commercially available carbohydrates and the ability to create a unique steric environment using different protecting groups should allow for the creation of carbohydrate-based catalysts which are more stereoselective.

Conclusions

Olefin metathesis catalysts incorporating carbohydrate-based NHCs have been synthesized and their structural characteristics and reactivity evaluated.

These complexes are characterized by a relatively rigid structure due to the steric bulk of the carbohydrate, and in contrast to many *N*-alkyl NHCs, show excellent stability and good reactivity in a variety of olefin metathesis reactions including ROMP, RCM, CM, and AROCM. Furthermore, they also show surprising selectivity in CM compared to other catalysts, confirming that steric bulk plays a large role in influencing olefin geometry. Similarly, observable levels of enantioselectivity due to the chiral nature of the carbohydrate were also demonstrated. These results demonstrate the viability of using carbohydrate NHCs in olefin metathesis and establish them as a unique structural class of ligand. Finally, with the potential of carbohydrate–based NHCs in olefin metathesis proven, further improvements in catalyst activity and selectivity via modification of the sugar (steric) and NHC backbone (electronic) should be possible.

Experimental

All reactions were carried out in dry glassware under an argon atmosphere using standard Schlenk techniques or in a Vacuum Atmospheres Glovebox under a nitrogen atmosphere unless otherwise specified. All solvents were purified by passage through solvent purification columns and further degassed with argon. NMR solvents were dried over CaH_2 and vacuum transferred to a dry Schlenk flask and subsequently degassed with argon. Commercially available reagents were used as received unless otherwise noted. Silica gel used for the purification of organometallic compounds was obtained from TSI Scientific, Cambridge, MA (60 Å, pH 6.5–7.0).

2D-NMR experiments were conducted on a Varian 600 MHz spectrometer equipped with a Triax (1H, 13C, 15N) probe while VT and kinetic experiments were

conducted on a Varian 500 MHz spectrometer equipped with an AutoX probe. Accurate temperature measurements of the NMR probe were obtained using a thermocouple connected to a multimeter with the probe immersed in an NMR tube containing toluene. Experiments and pulse sequences from Varian's Chempack 4 software were used without modification except for changes in the number of FIDs and scans per FID. Reaction conversions were obtained by comparing the integral values of starting material and product, no internal standard was used. Chemical shifts are reported in ppm downfield from Me_4Si by using the residual solvent peak as an internal standard. Spectra were analyzed and processed using MestReNova Ver. 5.2.5–4119.

Preparation of A.2b: Mesityl imidazole[29] (1.06 g, 5.67 mmol), **A.1b** (2.57 g, 6.24 mmol), and AgOTf (1.60 g, 6.24 mmol) were placed in a dry 100 ml RB flask under argon and dissolved in 30 ml of dry MeCN. The RB was shielded from light and heated to 50 °C for 16 h. The reaction was cooled to 25 °C and the solution filtered through a pad of celite washing with MeCN then concentrated *in vacuo*. The resulting residue was dissolved in CH_2Cl_2 and MTBE was added until the solution became slightly cloudy. After cooling to –5 °C, an oily residue crashed out. The supernatant was removed and the oil was triturated with cold hexanes and concentrated to a light brown powder (1.8 g, 47%). **A.2b** was recovered as a 1.3:1 mixture of β:α anomers and used without further purification. ^{1}H NMR ($CDCl_3$, 300 MHz): δ 9.39 (s, 1H), 8.69 (s, 1H), 7.91 (s, 1H), 7.77 (s, 1H), 7.31 (s, 1H), 7.18 (s, 1H), 7.02 (s, 4H), 6.37 (m, 1H), 5.57 (m, 1H), 5.36 (m, 3H), 4.48 (t, J = 6.18 Hz, 1H), 4.19–4.03 (m, 4H), 2.18–1.97 (m, 42H).

Preparation of A.4a: In a glovebox, a 100 ml RB was charged with **A.3** (0.497 g, 0.604 mmol), **A.2a** (0.604 g, 0.906 mmol), and NaO^{t}Bu (0.087 g, 0.906 mmol). 50 ml of dry THF was added and the reaction was stirred for 1 h at 25 °C after which it was removed from the glovebox and conc. in vacuo. The residue was dissolved in a minimal amount of CH_2Cl_2, loaded onto a column of TSI silica gel, and eluted with 10% diethyl ether/pentane to first collect excess **A.3** as a dark purple band, followed by 30% ether/pentane, and finally 60% ether/pentane until a dark pink/ red band was collected. After concentration of the relevant fractions, a dark pink residue was obtained which could be lyophilized from benzene to yield **A.4a** (208 mg, 33%) as a dark pink powder. ^{1}H NMR (C_6D_6, 600 MHz, major isomer): δ 19.74 (s, 1H), 8.4–7.8 (br s, 2H), 7.10 (d, J = 1.8 Hz, 1H), 6.95 (m, 3H), 6.31 (br s, 1H), 6.03 (d, J = 1.8 Hz, 1H), 5.98 (br s, 1H), 5.94 (t, J = 9 Hz, 1H), 5.88 (t, J = 9.6 Hz, 1H), 5.57 (t, J = 9.6 Hz, 1H), 4.39 (m, 2H), 4.26 (ad, J = 10.8 Hz, 1H), 2.53 (m, 3H), 2.23 (s, 6H), 1.98 (br s, 3H), 1.88 (br s, 6H), 1.80 (br s, 12H), 1.73 (m, 9H), 1.59 (m, 6H), 1.23 (m, 9H). ^{13}C NMR (151 MHz, C_6D_6) δ 298.0, 192.6, 170.39, 170.22, 169.94, 152.44, 138.70, 137.03, 136.86, 136.51, 129.46, 129.14, 128.90, 124.55, 124.54, 120.36, 120.34, 87.17, 75.50, 74.74, 71.13, 69.30, 62.00, 33.17, 33.06, 30.49, 28.52, 28.49, 28.46, 28.43, 27.24, 21.42, 21.31, 20.94, 20.55, 20.53, 18.97, 18.69. ^{31}P NMR (202 MHz, C_6D_6) δ 30.86 (major), 28.17 (minor). HRMS (FAB+) Calculated—1058.332, Experimental—1058.329.

Preparation of A.4b: An analogous procedure to that of **A.4a** was followed yielding **A.4b** (17%) as a 1.2:1 mixture of anomers. ^{1}H NMR (C_6D_6, 600 MHz, major isomer): δ 19.78 (s, 1H), 8.4–7.9 (br s, 4H), 7.46 (d, J = 1.56 Hz, 1H), 7.06

(d, J = 5.1 Hz, 1H), 6.95 (br t, J = 7.38 Hz, 2H), 6.76 (d, J = 3.54 Hz, 1H), 6.32 (br s, 1H), 6.27 (t, J = 9.48 Hz, 1H), 6.03 (d, J = 2.04 Hz, 1H), 6.00 (br s, 1H), 5.91 (d, J = 2.88 Hz, 1H), 5.82 (m, 1H), 5.71 (m, 1H), 5.67 (m, 1H), 5.63 (m, 1H), 4.64 (br t, J = 6.78 Hz, 1H), 4.38 (m, 1H), 4.22 (m, 1H), 4.17 (m, 1H), 4.10 (m, 2H), 2.54 (m, 6H), 2.26 (s, 6H), 1.98–1.55 (m, 77H), 1.24 (m, 15H). ^{13}C NMR (151 MHz, C_6D_6) δ 193.04, 170.52, 170.37, 170.35, 170.20, 170.13, 169.94, 169.92, 169.81, 168.82, 152.49, 138.71, 137.09, 136.88, 136.52, 129.46, 129.17, 128.66, 128.61, 128.53, 128.45, 128.37, 128.29, 128.21, 128.10, 124.60, 124.59, 120.54, 120.52, 92.94, 90.54, 87.65, 74.31, 72.66, 72.22, 71.67, 69.65, 68.86, 68.55, 68.25, 68.17, 68.03, 67.57, 67.51, 61.69, 61.47, 61.21, 33.08, 33.04, 32.97, 30.51, 30.49, 30.37, 30.15, 28.54, 28.51, 28.49, 28.44, 28.43, 27.60, 27.28, 27.16, 27.01, 21.58, 21.32, 20.73, 20.63, 20.53, 20.52, 20.49, 20.47, 20.43, 20.41, 20.39, 20.24, 20.18, 19.01, 18.67. ^{31}P NMR (121 MHz, C_6D_6) δ 31.19 (major), 28.53 (minor). HRMS (FAB+) Calculated—1057.324, Experimental—1057.321.

Representative procedure for ROMP/RCM kinetics: In a glovebox, catalyst **A.4a** (2.5 mg, 0.0024 mmol) was dissolved in CD_2Cl_2 (0.8 ml) and placed in a NMR tube equipped with a rubber septum. The NMR tube was removed from the glovebox and COD (distilled prior to use) (30 µL, 0.24 mmol) was injected after which the tube was immediately placed in the spectrometer and a spectral array started by arraying the “pad” variable for Varian spectrometers.

Representative procedure for CM Kinetics: Allyl benzene and cis-diacetoxybutene were distilled prior to use. In a glovebox, a scintillation vial was charged with allyl benzene (20 µL, 0.153 mmol), cis-diacetoxybutene (49 µL, 0.305 mmol), and

tridecane standard (50 µL, 0.205 mmol). CH_2Cl_2 (0.75 ml) was added followed by **A.4a** (4 mg, 0.004 mmol) as a solution in CH_2Cl_2. The vial was equipped with a septa top, removed from the glovebox and stirred under argon. Aliquots were removed via syringe at the specified time points and added to a GC vial containing a solution of ethyl vinyl ether in CH_2Cl_2 in order to quench the catalyst. GC retention times were as follows (min): allyl benzene (10.87), tridecane (11.55), cis-diacetoxybutene (18.13), trans-diacetoxybutene (18.70), cis-12 (21.27), trans-12 (21.48), trans-homocoupled allyl benzene (24.09), cis-homocoupled allyl benzene (24.34).

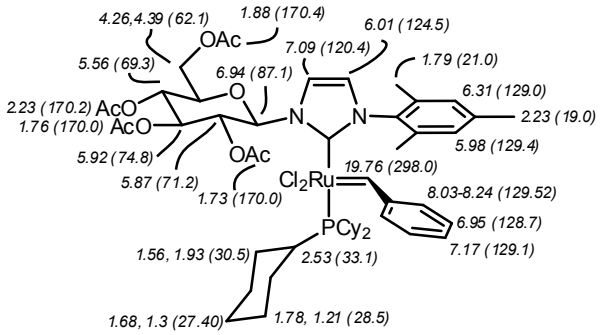

Figure A.9. ^{1}H (^{13}C) assignments for major isomer of catalyst **A.4a** based on spectroscopic data

Representative procedure for AROCM: A 10 ml RB was dried and charged with the norbornene substrate (0.109 mmol), styrene (0.125 mL, 1.09 mmol) which had been passed through a small plug of silica gel, and dry toluene (2 mL). Catalyst **A.4a** (6 mg, 0.005 mmol) was injected as a solution in toluene and the reaction stirred at 40°C for 14 h. The solvent was evaporated and the remaining residue was purified by flash chromatography to yield the desired product. Chromatography and HPLC conditions for all compounds studied have been previously reported.[30]

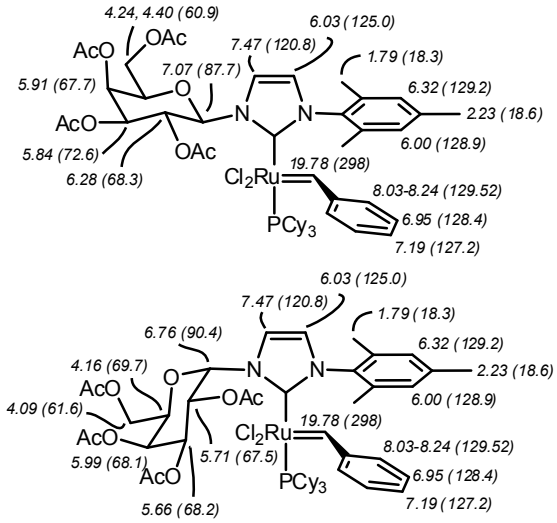

Figure A.10. ^{1}H (^{13}C) assignments β (top) and α (bottom) anomers of **A.4b**

Measurement of benzylidene rotation rate using line shape analysis: A lineshape analysis of the benzylidene rotation in **A.4a** was performed in order to obtain a more accurate estimate of $\Delta G^{\ddagger}$. The coalescence temperature could not be reached due to catalyst decomposition, however, a suitable temperature range from 12.5–73.1 °C was found in which there was no observable catalyst decomposition. To measure the rate of benzylidene rotation, **A.4a** was dissolved in ca. 0.6 mL of dry C_6D_6 and placed into a J. Young tube inside of a glove box. The tube was sealed and removed from the box and placed inside the spectrometer where it was allowed to equilibrate at the appropriate temperature for ca. 10 min before acquisition. The probe was calibrated at each temperature according to the method described in the General Information. Each experiment was run with ^{31}P decoupling in order to simplify the line shape analysis of the resulting spectrum. Experimental spectra were simulated using the MEXICO set of programs developed by Professor Alex Bain.[31] The noniterative version of MEXICO was used through

the SpinWorks (Ver. 3) NMR program which overlays the MEXICO simulation with the experimental spectrum and calculates an RMS value immediately.[32]

References

(1) (a) Van Veldhuizen, J. J.; Garber, S. B.; Kingsbury, J. S.; Hoveyda, A. H. *J. Am. Chem. Soc.* **2002**, *124*, 4954. (b) Despagnet-Ayoub, E.; Grubbs, R. H. *Organometallics* **2005**, *24*, 338. (c) Weigl, K.; Kohler, K.; Dechert, S.; Meyer, F. *Organometallics* **2005**, *24*, 4049. (d) Funk, T. W.; Berlin, J. M.; Grubbs, R. H. *J. Am. Chem. Soc.* **2006**, *128*, 1840. (e) Vehlow, K.; Maechling, S.; Blechert, S. *Organometallics* **2006**, *25*, 25. (f) Anderson, D. R.; Lavallo, V.; O'Leary, D. J.; Bertrand, G.; Grubbs, R. H. *Angew. Chem. Int. Ed.* **2007**, *46*, 7262. (g) Berlin, J. M.; Campbell, K.; Ritter, T.; Funk, T. W.; Chlenov, A.; Grubbs, R. H. *Org. Lett* **2007**, *9*, 1339. (h) Stewart, I. C.; Ung, T.; Pletnev, A. A.; Berlin, J. M.; Grubbs, R. H.; Schrodi, Y. *Org. Lett* **2007**, *9*, 1589. (i) Chung, C. K.; Grubbs, R. H. *Org. Lett* **2008**, *10*, 2693. (j) Vougioukalakis, G. C.; Grubbs, R. H. *J. Am. Chem. Soc.* **2008**, *130*, 2234.

(2) Kuhn, K. M.; Bourg, J. B.; Chung, C. K.; Virgil, S. C.; Grubbs, R. H. *J. Am. Chem. Soc.* **2009**, *131*, 5313.

(3) Schuster, O.; Yang, L.; Raubenheimer, H. G.; Albrecht, M. *Chem. Rev.* **2009**, *109*, 3445.

(4) (a) Weskamp, T.; Kohl, F. J.; Hieringer, W.; Gleich, D.; Herrmann, W. A. *Angew. Chem. Int. Ed.* **1999**, *38*, 2416. (b) Ledoux, N.; Allaert, B.; Linden, A.; Van Der Voort, P.; Verpoort, F. *Organometallics* **2007**, *26*, 1052. (c) Boydston, A. J.; Xia, Y.; Kornfield, J. A.; Gorodetskaya, I. A.; Grubbs, R. H. *J. Am. Chem. Soc.* **2008**, *130*,

12775.

(5) Savoie, J.; Stenne, B.; Collins, Shawn K. *Adv. Syn. Catal.* **2009**, *351*, 1826.

(6) Hudlicky, T.; Entwistle, D. A.; Pitzer, K. K.; Thorpe, A. J. *Chem. Rev.* **1996**, *96*, 1195.

(7) (a) Gamblin, D. P.; Scanlan, E. M.; Davis, B. G. *Chem. Rev.* **2008**, *109*, 131. (b) Murrey, H. E.; Hsieh-Wilson, L. C. *Chem. Rev.* **2008**, *108*, 1708.

(8) Dieguez, M.; Pamies, O.; Claver, C. *Chem. Rev.* **2004**, *104*, 3189.

(9) Hollingsworth, R. I.; Wang, G. *Chem. Rev.* **2000**, *100*, 4267.

(10) (a) Gyurcsik, B.; Nagy, L. *Coord. Chem. Rev.* **2000**, *203*, 81. (b) Steinborn, D.; Junicke, H. *Chem. Rev.* **2000**, *100*, 4283.

(11) (a) Nishioka, T.; Shibata, T.; Kinoshita, I. *Organometallics* **2007**,*26*, 1126. (b) Tewes, F.; Schlecker, A.; Harms, K.; Glorius, F. *J. Organomet. Chem.* **2007**, *692*, 4593. (c) Shi, J. C.; Lei, N.; Tong, Q. S.; Peng, Y. R.; Wei, J. F.; Jia, L. *Eur. J. Inorg. Chem.* **2007**, 2221.

(12) Determined by ^{1}H NMR spectrum analysis of J_{HH} coupling in **A.4b**.

(13) The silver complex was formed via deprotonation by silver (I) oxide. See ref. 11b for details.

(14) Unfortunately, in our hands, this methodology could not be extended to gluco- or galactopyransoyl bromides protected with benzyl (Bn), benzoyl (Bz), pivolate (Piv), or methyl (Me) groups. Attempts to form a phosphine-free catalyst via incorporation of a Hoveyda-type chelating benzylidene either by direct phosphine substitution or via cross metathesis of **A.4a/b** with β-methyl isoprepoxy styrene were also unsuccessful.

(15) (a) Oskam, J. H.; Fox, H. H.; Yap, K. B.; McConville, D. H.; Odell, R.; Lichtenstein, B. J.; Schrock, R. R. *J. Organomet. Chem.* **1993**, *459*, 185. (b) Oskam, J. H.; Schrock, R. R. *J. Am. Chem. Soc.* **1993**, *115*, 11831.

(16) (a) Grisi, F.; Costabile, C.; Gallo, E.; Mariconda, A.; Tedesco, C.; Longo, P. *Organometallics* **2008**, *27*, 4649. (b) Sanford, M. Ph.D. Thesis, California Institute of Technology, Pasadena, 2001

(17) A 2D-NOESY experiment conducted at −75 °C with a mixing time of 500 ms showed no exchange between the benzylidene rotamers (doublet and singlet) but small cross peaks between the two singlet resonances indicated that rotation about the Ru-NHC bond is not completely frozen out at this temperature. A low temperature VT-NMR experiment and subsequent line shape analysis yielded a $\Delta G^{\ddagger}$ consistent with previous reports of NHC rotation (see ref. 16b), although we cannot completely rule out another process such as oxygen coordination/ decoordination at this time. See Supporting Information for relevant spectra and plots.

(18) Although it is tempting to theorize that an oxygen from either an acetate or the sugar is coordinating to the metal center, we found no obvious indications of this during our NMR studies.

(19) Sandström, J.; *Dynamic NMR Spectroscopy*, Academic Press Inc.: New York, New York, 1982; pp. 53-54.

(20) See the experimental section details.

(21) At this time, we have been unable to synthesize a saturated variant of **A.4a** or **A.4b**.

(22) Love, J. A.; Sanford, M. S.; Day, M. W.; Grubbs, R. H. *J. Am. Chem. Soc.* **2003**, *125*, 10103.

(23) The kinetic plots shown were reproducible for different kinetic runs and also for different batches of catalyst.

(24) (a) Hong, S. H.; Wenzel, A. G.; Salguero, T. T.; Day, M. W.; Grubbs, R. H. *J. Am. Chem. Soc.* **2007**, *129*, 7961. (b) Hong, S. H.; Chlenov, A.; Day, M. W.; Grubbs, R. H. *Angew. Chem. Int. Ed.* **2007**, *46*, 5148.

(25) Flook, M. M.; Jiang, A. J.; Schrock, R. R.; Mueller, P.; Hoveyda, A. H. *J. Am. Chem. Soc.* **2009**, *131*, 7962.

(26) Ritter, T.; Hejl, A.; Wenzel, A. G.; Funk, T. W.; Grubbs, R. H. *Organometallics* **2006**, *25*, 5740.

(27) Kuhn, K. M.; Bourg, J. B.; Chung, C. K.; Virgil, S. C.; Grubbs, R. H. *J. Am. Chem. Soc.* **2009**, *131*, 5313.

(28) (a) Van Veldhuizen, J. J.; Garber, S. B.; Kingsbury, J. S.; Hoveyda, A. H. *J. Am. Chem. Soc.* **2002**, *124*, 4954. (b) Van Veldhuizen, J. J.; Gillingham, D. G.; Garber, S. B.; Kataoka, O.; Hoveyda, A. H. *J. Am. Chem. Soc.* **2003**, *125*, 12502. (c) Berlin, J. M.; Goldberg, S. D.; Grubbs, R. H. *Angew. Chem. Int. Ed.* **2006**, *45*, 7591.

(29) Ketz, B. E.; Cole, A. P.; Waymouth, R. M. *Organometallics* **2004**, *23*, 2835.

(30) Berlin, J. M.; Goldberg, S. D.; Grubbs, R. H. *Angew. Chem. Int. Ed.* **2006**, *45*, 7591.

(31) http://chemistry.mcmaster.ca/faculty/bain/

(32) Marat, Kirk. SpinWorks. http://www.umanitoba.ca/chemistry/nmr/spinworks/

index.html